COMMUNICATION

Ultrathin Direct Atomic Layer Deposition on Composite Electrodes for Highly Durable and Safe Li-Ion Batteries

By *Yoon Seok Jung, Andrew S. Cavanagh, Leah A. Riley, Sun-Ho Kang, Anne C. Dillon, Markus D. Groner, Steven M. George,* and *Se-Hee Lee**

In order to employ Li-ion batteries (LIBs) in next-generation hybrid electric and/or plug-in hybrid electric vehicles (HEVs and PHEVs), LIBs must satisfy many requirements: electrodes with long lifetimes (fabricated from inexpensive environmentally benign materials), stability over a wide temperature range, high energy density, and high rate capability. Establishing long-term durability while operating at realistic temperatures (5000 charge-depleting cycles, 15 year calendar life, and a range from −46 °C to +66 °C) for a battery that does not fail catastrophically remains a significant challenge.[1]

Recently, surface modifications of electrode materials have been explored as viable paths to improve the performance of LIBs for vehicular applications.[2] The cycle life and safety issues have been largely satisfied for Li_xMO_2 (M = Co, Ni, Mn, etc.) cathodes by coating the active material particles with a metal oxide and/or metal phosphate.[2a,2b,3] For anode, state-of-the-art materials such as Si suffer from significant volume expansion/contraction during charge–discharge leading to rapid capacity fade.[4] Natural graphite (NG) is a realistic candidate anode, for vehicular applications, due to its high reversible capacity, low and flat potential relative to Li/Li^+, moderate volume change, and low cost.[5] In previous reports, the performance of NG was improved by surface modifications with mild oxidation,[6] coating with amorphous carbon,[5c] metal oxides (Al_2O_3, ZrO_2),[5a,7] and metal phosphate ($AlPO_4$).[5b] These efforts were performed in order to mitigate the solid electrolyte interphase (SEI)[8] that is formed on the NG surface by reductive decomposition of the electrolyte during initial charge–discharge especially at elevated temperatures. The decomposition of the SEI at elevated temperature (~80 °C) is exothermic and initiates thermal runaway.[9] In most previous reports films of metal oxides and metal phosphates have been deposited on powder electrode materials with 'sol–gel' wet-chemical methods.[2a,2b,3,5,7] Unfortunately, sol-gel methods require large quantities of solvents as well as multiple complex steps. Also, these chemical techniques may only be employed for powders (i.e., a fully fabricated electrode cannot be coated).

Here we clearly demonstrate that conformal ultrathin protective coating by inactive metal oxide without disrupting inter-particle electronic pathway can be realized by atomic layer deposition (ALD) directly performed on a composite electrode, which leads to significant improvement of both long-term durability and safety of NG anode. Also ALD coatings are significantly more promising than efforts that have been previously reported.

Atomic layer deposition is a well established method to apply conformal thin films on high-surface area tortuous networks using sequential, self-limiting surface reactions.[10] Also, the thickness of ALD coatings is easily tailored at the atomic level (Å-level control). Recently, we reported that Al_2O_3-coated $LiCoO_2$ electrodes display superior electrochemical performance in comparison to $LiCoO_2$ electrodes that were not coated with ALD.[11] We employed a simple, well-known ALD process utilizing trimethylaluminium (TMA) and H_2O as precursors:[12]

$$(A)\quad AlOH^* + Al(CH_3)_3 \rightarrow AlO - Al(CH_3)_2^* + CH_4 \qquad (1)$$

$$(B)\quad AlCH_3^* + H_2O \rightarrow Al - OH^* + CH_4 \qquad (2)$$

The performance of both of these steps constitutes one ALD cycle.

In all of the previous efforts to apply protective coatings, the coatings were applied to powders, that then comprise the active material in the electrode, but not directly on the composite electrode, containing conductive additive and binder.[2a,2b,3,5,7]

[*] Prof. S. H. Lee, Dr. Y. S. Jung,[+] L. A. Riley
Department of Mechanical Engineering, University of Colorado at Boulder
Boulder, CO 80309-0427 (USA)
E-mail: sehee.lee@colorado.edu
[+] Present address: National Renewable Energy Laboratory, Golden, CO 80401 (USA)
Prof. S. M. George
Department of Chemistry and Biochemistry and Department of Chemical and Biological
Engineering, University of Colorado at Boulder
Boulder, CO 80309-0215 (USA)
Dr. S. H. Kang
Argonne National Laboratory
Argonne, IL 60439 (USA)
Mr. A. S. Cavanagh
Department of Physics, University of Colorado at Boulder
Boulder, CO 80309-0215 (USA)
Dr. A. C. Dillon
National Renewable Energy Laboratory
Golden, CO 80401 (USA)
Dr. M. D. Groner
ALD NanoSolutions Inc., 580 Burbank St., Unit 100
Broomfield, CO 80020 (USA)

DOI: 10.1002/adma.200903951

(Commercial LIBs are comprised of composite electrodes containing an active Li-ion insertion/extraction compound, carbon as a conductive additive, and a polymeric binder.) We have demonstrated that applying a conformal coating directly to the electrode is critical to achieving optimal electrochemical performance for LIB vehicular applications.

Figure 1a displays a scanning electron microscopy (SEM) cross-sectional image of a NG composite electrode following 5 cycles of Al_2O_3 ALD. The cross section was fabricated with focused ion beam (FIB) gallium milling. As depicted in Fig. 1a, the electrode is very porous. Seven regions of the electrode were analyzed with energy dispersive spectroscopy (EDS) to acquire elemental analysis data. Fig. 1b is a plot of the weight fraction of Al (Al/(C + Cu + Al)) as a function of the EDS depth profile in the NG composite electrode. Note, the Al content remains constant throughout the NG electrode (regions 1–6) and is negligible on the face of the Cu foil (region 7). The absence of the Al on the surface of the Cu foil and the relatively constant concentration of Al demonstrates that the Al is deposited conformally with ALD and not inadvertently sputter deposited during the FIB process. This was also confirmed by employing FIB milling to sputter through the Cu foil from the backside of the electrode. It was then possible to detect Al at only the Cu/NG interface. This conclusively shows that ALD precursors can diffuse through the pores of composite electrodes to deposit a conformal Al_2O_3 film in the torturous path of the entire electrode structure.

As discussed in more detail below, we have also demonstrated that in most cases it is critical to apply an ALD coating directly to a fabricated electrode rather than to powders of active materials. We believe that when ALD is performed directly on powders, slower Li-ion diffusion as well as e^- transport through the Al_2O_3 layer is observed. Conversely when ALD is employed on the composite electrode the Al_2O_3 is not deposited at contact points between active material particles and the current collector, maintaining electrical conductivity and enabling rapid electron transport. Figure 2a displays a schematic representation of Li-ion and electron transport through $LiCoO_2$ particles in an electrode fabricated from ALD coated powders and an ALD coated composite electrode.

Figure 2b compares the charge–discharge voltage profiles of bare $LiCoO_2$ and $LiCoO_2$ (commercial cathode technology) coated with 20 cycles of ALD on the powder and also directly on the electrode. The additional overpotential ('∧') with respect to bare $LiCoO_2$ for ALD on the powder is larger than that observed ('*') for ALD directly on the electrode. The difference between the overpotential of the ALD on the powder and the ALD directly on the electrode may be attributed to the hindrance of e^- transport in the Al_2O_3 film resulting from the complete ALD coverage on the active material powder. Figure 2b also suggests that the kinetics is actually improved by growing the ALD Al_2O_3 film directly on the composite electrode.

Typically the first ALD Al_2O_3 reaction requires a hydroxyl-terminated surface, which is present on metal oxides. However, the conjugated carbon bonds in the graphitic planes of NG are relatively inert. Thus in order to perform ALD on the

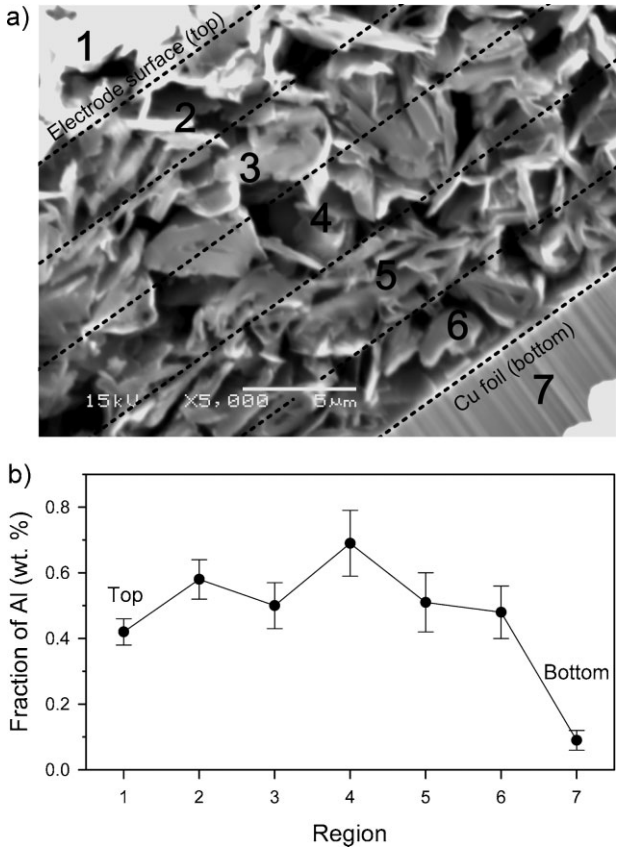

Figure 1. SEM/EDS analyses of Al_2O_3 ALD electrodes. a) FE-SEM cross-sectional image of a NG composite electrode coated with 5 cycles of Al_2O_3 ALD. Numbers indicate regions in which Al was analysed with EDS. b) Weight fraction of Al as a function of depth.

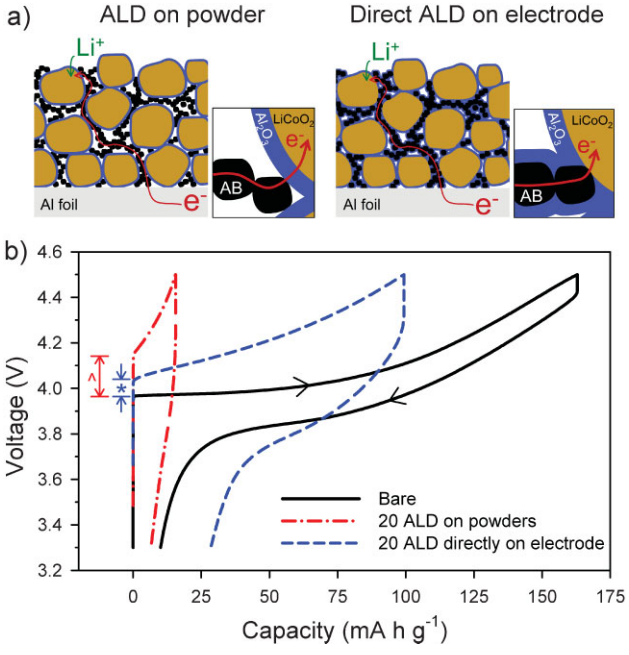

Figure 2. a) Schematics of transport in $LiCoO_2$ composite electrodes when ALD is performed first on the powder versus when ALD is performed directly on the composite electrode. b) Charge–discharge curves at 1 C-rate (140 mA g^{-1}) at room temperature. Note the polarization increase ('∧' and '*') observed for Al_2O_3 coatings with respect to the curve for bare $LiCoO_2$.

NG surface, it was necessary to pre-treat the NG with NO_2 prior to TMA exposure:[13]

$$(A)\quad NG^{*} + NO_2 \rightarrow NG - NO_2^{*} \tag{3}$$

$$(B)\quad NG - NO_2^{*} + TMA \rightarrow NG - NO_2^{*} - TMA^{*} \tag{4}$$

Following this process, the NO_2 nitrogen behaves as a Lewis base and is attached to the NG surface via strong van der Walls interactions leaving oxygen atoms accessible to reaction with TMA. In order to demonstrate the effect of the NO_2 pretreatment, Al_2O_3 ALD on NG was performed with and without NO_2 pretreatment. The electronic conductivity was then measured for each sample to verify thickness and conformity of the ALD coating (Supplementary Fig. S1). As expected, the ALD Al_2O_3 coated NG showed decreased conductivity with increasing number of ALD cycles, and the NO_2 pretreated NG was less conductive than non-treated NG.

Furthermore, NG electrodes prepared with Al_2O_3 ALD coatings on powder and also directly on the electrodes were tested using charge–discharge cycling at a highly elevated temperature of 50 °C. As a control sample, bare NG was also tested at 50 °C. The bare NG displays a relatively rapid decay in reversible capacity versus the number of charge–discharge cycles (Fig. 3a), attributed to instability of a SEI layer.[8c] Conversely, the capacity retention is dramatically improved by performing only 5 cycles Al_2O_3 ALD directly on the electrode. Highly improved electrochemical performance was obtained both with and without the use of a NO_2 surface nucleation pretreatment. The charge–discharge capacity retention for the electrode coated with 5 Al_2O_3 ALD cycles with NO_2 is 98% for 200 charge–discharge cycles, normalized to the reversible capacity at the 3rd charge–discharge cycle, with negligible kinetic hindrance. Surprisingly, the electrode coated with 5 cycles Al_2O_3 ALD without NO_2 pretreatment also displayed excellent capacity stability indicating that the NG must have enough edge and/or defective sites to allow for TMA nucleation. The improved cycle life achieved via ALD directly on the electrode is believed to result from a stable 'artificial' thin film SEI of Al_2O_3 that protects the NG surface from undesirable decomposition reactions with the electrolyte.

Table 1. Cycle performance of Al_2O_3-coated NG electrodes.

Temperature	ALD[a]		Capacity retention [%] [c]	
	Cycle number	NO_2/TMA[b]	100th	200th
RT	Bare		90	80
RT	2	No	100	99
RT	5	No	104	102
RT	5	Yes	104	103
50 °C	Bare		53	26
50 °C	2	No	96	88
50 °C	5	No	97	93
50 °C	5	Yes	99	96

[a] Al_2O_3 ALD was done on NG electrodes. [b] Al_2O_3 ALD was done after 10 cycles of NO_2/TMA pretreatment. [c] Capacity retention of the reversible capacity at given charge–discharge cycle with respect to that at the 3rd charge–discharge cycle.

In an extensive comparison of the charge–discharge cycle retention relative to the number of ALD cycles for samples with and without the NO_2 pretreatment, thicker conformal coatings exhibit slightly better electrochemical performance (Table 1). At room temperature, ALD Al_2O_3 coated NG also exhibits excellent cycling retention with negligible kinetic limitations (Supporting Information, Fig. S2). When compared with the previous results obtained from NG coated by wet chemical methods (Table S1), ALD-coated NG delivers much more promising performance even at elevated temperature (50 °C).

In contrast with the Al_2O_3 ALD coating on the NG electrode, Fig. 3a shows that NG particles coated with 5 cycles of Al_2O_3 ALD, subsequently fabricated into electrodes, display significantly decreased capacity retention compared to bare NG. The degradation in performance is attributed to the insulating property of the Al_2O_3 film. The insulating Al_2O_3 layer inhibits electron conduction paths between NG particles and the current collector. A schematic of this effect is illustrated in Fig. 3b. We also note that NG experiences an ~13% volume change during a charge–discharge cycle.[14] For the ALD powder, the NG particles and the current collector are isolated by the insulating Al_2O_3 film and therefore even a slight volume change in the NG disrupts the electrical conductivity between the particles and current collector. The repeated volume expansion and contraction subsequently accelerates loss of electronic conduction pathways. Importantly, ALD performed directly on the electrode enables the electrical pathways between particles to not be coated with an insulating layer allowing for necessary conductivity (Fig. 3b).

The irreversible capacity observed upon the first charge is undoubtedly attributed to the

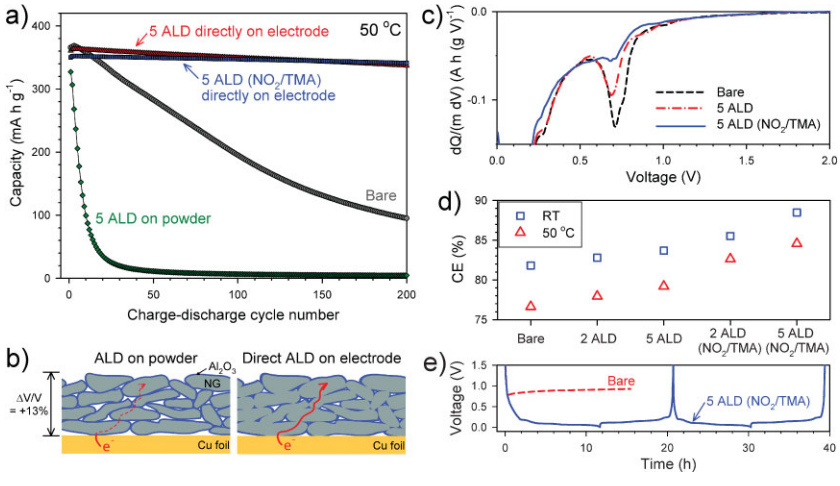

Figure 3. Electrochemical performance for ALD coated NG composite electrodes. a) Cycle performance at 50 °C. b) Schematic representation transport in NG composite electrodes prepared by ALD on powder and ALD directly on the electrode. c) Differential first charge voltage profiles at room temperature. d) Coulombic efficiency (CE) at the first charge–discharge cycle. e) Voltage profiles at room temperature when using 1 M $LiPF_6$ in PC as electrolyte.

formation of an SEI layer.[8,15] However, this large irreversible reaction is undesirable because it results in large impedance and also causes loss of valuable Li^+ from the cathode material, which results in ultimately lower full cell capacity. The intensity of the differential charge peak at 0.7 V during the first charge (Fig. 3c) indicates that the irreversible reductive decomposition of the electrolyte decreases for NG coated with ALD Al_2O_3 and further decreases if the NO_2 pretreatment is employed (Bare > 5 ALD cycles > 5 ALD cycles with NO_2 pretreatment). Accordingly, the coulombic efficiency (CE), the ratio of discharge capacity to charge capacity, significantly increases (Fig. 3d) for the NO_2 treated sample. Furthermore, the conformal Al_2O_3 coating on the composite NG electrodes allows propylene carbonate (PC) to be employed as the electrolyte. Due to its low melting point (~49 °C)[5c] PC is essentially only employed for operating LIBs at low temperatures and is thus particularly important for cold weather operation of HEVs. The voltage plateau at 0.8 V for bare NG is indicative of electrochemical exfoliation by PC molecules.[5c,16] In contrast, NG electrodes coated with 5 cycles of Al_2O_3 ALD with the NO_2/TMA process allows for reversible Li^+ insertion/extraction without an irreversible plateau related to exfoliation (Fig. 3e) and importantly reveals stable cycling performance (Supplementary Fig. S3). Furthermore, PC-NG compatibility achieved by ALD confirms the conformity of the ALD coating and also suggests commercialization of ALD processes for a variety of electrode materials.

Figure 4 shows differential scanning calorimetry (DSC) curves of the fully lithiated bare NG electrode (dashed line) and NG electrode coated with 5 Al_2O_3 ALD cycles with the NO_2/TMA process (solid line) in the presence of electrolyte. The fully lithiated, ALD coated NG electrode exhibits significantly lower heat generation between 100–150 °C compared to bare NG electrodes. The heat generation in this temperature range is attributed to conversion of a meta-stable SEI to a more stable SEI layer or further electrolyte decomposition at the graphite surface, which may in turn significantly affect the LIB safety performance.[9] The results in Fig. 4 indicate that the SEI layer formed on the ALD coated NG electrode is smaller and/or more stable than that formed on bare NG electrodes, consistent with the results in Fig. 3c.

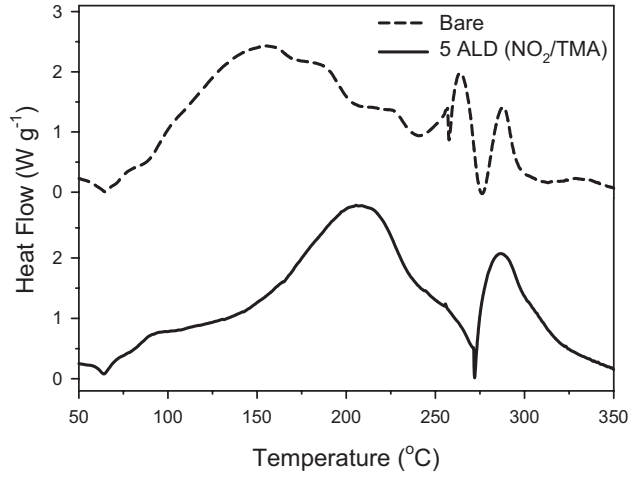

Figure 4. DSC curves of fully lithiated electrodes in the presence of electrolyte. Bare NG electrode (dotted line) and NG electrode coated with 5 Al_2O_3 ALD cycles with NO_2 pretreatment (solid line).

Finally, a $LiCoO_2$/NG full cell cycled in the 3.30–4.45 V range is provided in Supplementary Fig. S4. The full cell was made from $LiCoO_2$ coated with 2 cycles of ALD Al_2O_3 on powder and NG coated with 2 cycles of ALD Al_2O_3 on the electrode. The coated full cell shows a dramatically enhanced cycling performance.

In conclusion, we have demonstrated that ALD deposited directly on electrode surfaces may protect the surface of the active powders in electrodes while maintaining an interparticle electronic pathway. The anomalous cycling performance at elevated temperatures, PC-compatibility, and improved safety performance of Al_2O_3 coated NG composite electrodes suggests viability for next generation electric vehicles. Furthermore, the versatility of direct ALD on composite electrodes may be employed to develop coatings for any advanced battery materials.

Experimental

Atomic Layer Deposition: Al_2O_3 ALD films were grown directly on NG and $LiCoO_2$ particles using a rotary reactor. For the Al_2O_3 ALD, TMA (97%) and HPLC (high performance liquid chromatography) grade H_2O was obtained from Sigma-Aldrich. The typical growth rate for the chemistry is 1.1 Å per cycle [17]. However, due to the large surface area of the $LiCoO_2$ and NG powders, it is difficult to completely purge H_2O from the reactor. The presence of H_2O in the reactor during the TMA reaction leads to slightly enhanced growth per cycle resulting from some chemical vapor deposition.

The Al_2O_3 ALD reaction sequence was: i) TMA dose to 1.0 Torr; ii) evacuation of reaction products and excess TMA; iii) N_2 dose to 20.0 Torr; iv) N_2 static time; v) evacuation of N_2; vi) H_2O dose to 1.0 Torr, vii) evacuation of reaction products and excess H_2O; viii) dose N_2; and ix) evacuation of N_2 and any entrained gases. This sequence constitutes one AB cycle of Al_2O_3 ALD. ALD was conducted at 180 °C.

For the NO_2 nucleation treatment, commercial purity grade NO_2 (99.5%) was acquired from Airgas. In this work, 10 cycles of NO_2/TMA functionalized the NG. This NO_2/TMA functionalization was performed with the following sequence: i) exposure to NO_2 to set pressure; ii) evacuation of excess NO_2; iii) exposure to TMA to set pressure; and iv) TMA excess evacuation. This sequence defines one AB cycle of the NO_2/TMA functionalization layer.

Electrochemical Characterization: The $LiCoO_2$ composite electrode was prepared by spreading $LiCoO_2$ powder (7–10 μm, L106, LICO Technology), acetylene black (AB), and PVDF (polyvinylidene fluoride, binder) (83.0:7.5:9.5 weight ratio) on a piece of Al foil. The NG composite electrodes were composed of NG (~5 μm, HPM850, Asbury Graphite Mills Inc.) and PVDF (90:10 weight ratio) on Cu foil. Cells were assembled in an Ar-dry box and tested in a temperature-controlled oven. The galvanostatic charge–discharge cycling was performed in 2032-type coin cells. The $LiCoO_2$/Li cells were cycled between 3.3–4.5 V at 0.1 C-rate (14 mA g^{-1}) for the first two cycles and 1 C-rate for the subsequent cycles at room temperature. The NG/Li cells were cycled between 0.005–1.500 V at 0.1 C-rate (37 mA g^{-1}) for the first two cycles and 0.5 C-rate for subsequent cycles. $LiCoO_2$/NG full cells were cycled at 3.30–4.45 V, 0.1 C-rate (14 mA g^{-1} of $LiCoO_2$) for the first two cycles and 1 C for subsequent cycles. The weight ratio of $LiCoO_2$/NG was ~1.4. 1.0 M $LiPF_6$ dissolved in a mixture of ethylene carbonate (EC) and dimethyl carbonate (DMC) (1:1 v/v). As a separator, a glass fiber sheet and a porous 20 μm thick polypropylene (PP)/polyethylene/PP trilayer film were used for NG/Li and NG/$LiCoO_2$ cells, respectively.

Thermal Properties: Perkin-Elmer DSC experiment were conducted on fully lithiated bare NG electrodes and NG electrodes coated with 5 Al_2O_3 ALD cycles with NO_2 pretreatment. The scan rate and measurement temperature range were 10 °C min^{-1} and 50–350 °C, respectively. The fully

lithiated electrodes were prepared in lithium cells by cycling four times between 0.005 and 1.5 V at 0.063 mA cm^{-2} and charging to 0.005 V before DSC sample preparation. The electrolyte used for the DSC experiment was 1.2 M $LiPF_6$ in a mixture of EC and ethyl methyl carbonate (EMC) (3:7 wt %). The cells were disassembled and a portion of the fully charged electrode was scraped from the Cu current collector and hermetically sealed inside high-pressure stainless-steel crucibles. Preparation of the DSC samples was conducted in an Ar-filled dry box. An empty, sealed stainless-steel crucible was used for the reference pan of the calorimeter. The DSC measurement was duplicated for each sample to ensure reproducibility of the experimental data.

Acknowledgements

This work was funded by a subcontract from a DOE SBIR grant to ALD Nanosolutions. A.S.C. received additional support from the iMINT DARPA Center at the University of Colorado. Y.S.J. acknowledges the Korea Research Foundation Grant funded by [KRF-2008-357-D00066]. A.C.D. is grateful for support from the U.S. Department of Energy under subcontract number DE-AC36-08GO28308 through: DOE Office of Energy Efficiency and Renewable Energy Office of the Vehicle Technologies Program. S.-H.K. gratefully acknowledges support from the Office of FreedomCar and Vehicle Technologies of the U.S. Department of Energy. Supporting Information is available online from Wiley InterScience or from the author.

Received: November 19, 2009
Revised: December 12, 2009
Published online: April 6, 2010

[1] Idaho National Laboratory website, *Battery Test Manual for Plug-In Hybrid Electric Vehicle*, http://www.inl.gov (last accessed January 2010).
[2] a) J. Cho, Y. J. Kim, T. J. Kim, B. W. Park, *Angew. Chem. Int. Ed.* **2001**, *40*, 3367. b) J. Cho, Y. W. Kim, B. Kim, J. G. Lee, B. W. Park, *Angew. Chem. Int. Ed.* **2003**, *42*, 1618. c) A. S. Aricò, P. Bruce, B. Scrosati, J.-M. Tarascon, W. V. Schalkwijk, *Nat. Mater.* **2005**, *4*, 366. d) B. Kang, G. Ceder, *Nature* **2009**, *458*, 190.
[3] a) C. Li, H. P. Zhang, L. J. Fu, H. Liu, Y. P. Wu, E. Rahm, R. Holze, H. Q. Wu, *Electrochim. Acta* **2006**, *51*, 3872. b) Y. K. Sun, Y. S. Lee, M. Yoshio, K. Amine, *Electrochem. Solid-State Lett.* **2002**, *5*, A99.
[4] a) J. H. Ryu, J. W. Kim, Y. E. Sung, S. M. Oh, *Electrochem. Solid-State Lett.* **2004**, *7*, A306. b) Y. S. Jung, K. T. Lee, J. H. Kim, J. Y. Kwon, S. M. Oh, *Adv. Funct. Mater.* **2008**, *18*, 3010.
[5] a) S. S. Kim, Y. Kadoma, H. Ikuta, Y. Uchimoto, M. Wakihara, *Electrochem. Solid-State Lett.* **2001**, *4*, A109. b) S. E. Lee, E. Kim, J. Cho, *Electrochem. Solid-State Lett.* **2007**, *10*, A1. c) M. Yoshio, H. Wang, K. Fukuda, *Angew. Chem. Int. Ed.* **2003**, *42*, 4203.
[6] C. Menachem, E. Peled, L. Burstein, Y. Rosenberg, *J. Power Sources* **1997**, *68*, 277.
[7] a) I. R. M. Kottegoda, Y. Kadoma, H. Ikuta, Y. Uchimoto, M. Wakihara, *J. Electrochem. Soc.* **2005**, *152*, A1595. b) I. R. M. Kottegoda, Y. Kadoma, H. Ikuta, Y. Uchimoto, M. Wakihara, *Electrochem. Solid-State Lett.* **2002**, *5*, A275.
[8] a) E. Peled, *J. Electrochem. Soc.* **1979**, *126*, 2047. b) E. Peled, D. Golodnitsky, G. Ardel, *J. Electrochem. Soc.* **1997**, *144*, L208. c) H. L. Zhang, F. Li, C. Liu, J. Tan, H. M. Cheng, *J. Phys. Chem. B* **2005**, *109*, 22205.
[9] a) H. Yang, H. Bang, K. Amine, J. Prakash, *J. Electrochem. Soc.* **2005**, *152*, A73. b) T. Doi, L. Zhao, M. Zhou, S. Okada, J. Yamaki, *J. Power Sources* **2008**, *185*, 1380.
[10] a) M. Ritala, M. Leskela, *Handbook of Thin Film Materials*, Academic Press, San Diego, CA 2001. b) S. M. George, A. W. Ott, J. W. Klaus, *J. Phys. Chem.* **1996**, *100*, 13121. c) S. M. George, *Chem. Rev.* **2010**, *110*, 111.
[11] Y. S. Jung, A. S. Cavanagh, A. C. Dillon, M. D. Groner, S. M. George, S. H. Lee, *J. Electrochem. Soc.* **2010**, *157*, A75.
[12] A. C. Dillon, A. W. Ott, J. D. Way, S. M. George, *Surf. Sci.* **1995**, *322*, 230.
[13] a) D. B. Farmer, R. G. Gordon, *Nano Lett.* **2006**, *6*, 699. b) A. S. Cavanagh, C. A. Wilson, A. W. Weimer, S. M. George, *Nanotechnology* **2009**, *20*, 255602.
[14] Y. Koyama, T. E. Chin, U. Rhyner, R. K. Holman, S. R. Hall, Y. M. Chiang, *Adv. Funct. Mater.* **2006**, *16*, 492.
[15] a) R. Fong, U. V. Sacken, J. R. Dahn, *J. Electrochem. Soc.* **1990**, *137*, 2009. b) D. Aurbach, Y. Ein-Eli, O. Chusid, *J. Electrochem. Soc.* **1994**, *141*, 603.
[16] A. N. Dey, B. P. Sullivan, *J. Electrochem. Soc.* **1970**, *117*, 222.
[17] a) M. D. Groner, F. H. Fabreguette, J. W. Elam, S. M. George, *Chem. Mater.* **2004**, *16*, 639. b) A. W. Ott, J. W. Klaus, J. M. Johnson, S. M. George, *Thin Solid Films*, **1997**, *292*, 135.